detritus | Multidisciplinary Journal for Circular Economy and Sustainable Management of Residues

CISA

# UNLOCKING COPPER FROM ELECTRONIC WASTE: OPTIMIZED LEACHING STRATEGIES AND RAPID ANALYTICAL CHEMISTRY EVALUATION

Efe Olomu [1,2], Dennis Silva Ferreira [3], Edenir Rodrigues Pereira-Filho [3] and Fabiola Manhas Verbi Pereira [1,*]

[1] *Group of Alternative Analytical Approaches (GAAA), Bioenergy Research Institute (IPBEN), Institute of Chemistry, São Paulo State University (UNESP), Araraquara 14800-060, São Paulo State, Brazil*
[2] *University of Port Harcourt, East/West Road, PMB 5323, Choba, Rivers State, Nigeria*
[3] *Group of Applied Instrumental Analysis, Chemistry Department, Federal University of São Carlos, São Carlos 13565-905, São Paulo State, Brazil*

**Article Info:**
Received:
6 May 2025
Revised:
14 August 2025
Accepted:
10 September 2025
Available online:
30 September 2025

**Keywords:**
Electronic waste
Copper extraction
EDXRF
LIBS
Leaching

**ABSTRACT**

This study presents a novel method for evaluating copper (Cu) extraction efficiency by combining chemometric approaches with non-invasive analytical techniques, including Energy-Dispersive X-Ray Fluorescence (ED-XRF) and Laser-Induced Breakdown Spectroscopy (LIBS). Aligned with Process Intensification (PI) principles, our methodology utilizes the Design of Experiments (DoE) approach to streamline decision-making in metal recovery processes. While the in-situ generation of Cu ions in the liquid medium yielded suboptimal results, this approach warrants further investigation to optimize its potential. On the other hand, our findings demonstrate that LIBS and XRF are highly effective in differentiating leachates based on Cu signals, offering advantages such as higher analytical frequency and lower operational costs compared to traditional methods like Inductively Coupled Plasma Optical Emission Spectroscopy (ICP OES). These non-invasive techniques enhance process understanding, enabling more efficient and informed decision-making. By integrating PI with DoE, this study advances Cu recycling strategies from Waste Electrical and Electronic Equipment (WEEE), paving the way for more sustainable and cost-effective recovery processes. This approach holds significant promise for addressing the growing challenges of e-waste management and resource recovery.

## 1. INTRODUCTION

Electronic waste (e-waste) represents one of the fastest-growing and most pressing environmental challenges globally. Despite its severity, adequate collection and recycling initiatives remain limited in Brazil, other Latin American nations, and Nigeria. The associated logistics and treatment processes are highly complex, requiring substantial human resources and incurring considerable costs for selective collection, secure transportation, and waste processing. These constraints significantly hinder the feasibility of large-scale implementation (Lundgren, 2012).

Any electrical and electronic equipment (EEE) discarded by its owner with no intention of reuse is considered e-waste, also known as waste electrical and electronic equipment (WEEE). In 2022, approximately 62.0 million tons (Mt) of e-waste were generated worldwide. Of this amount, 14.0 Mt (around 23%) were produced in the Americas, with the United States leading at 7.2 Mt, followed by Brazil with 2.4 Mt (Baldé et al., 2024).

Why has e-waste generation increased annually? This can be attributed to rapid technological advancements, which introduce new devices with enhanced functionalities and a wider variety of options. As a result, the lifecycle of existing equipment has shortened significantly, often to just 1-2 years or even less (Lundgren, 2012; Andrade et al., 2019; Baldé et al., 2024). For instance, a smartphone is typically used for less than two years before being replaced by a more advanced model that offers new attributes. These technological advancements meet global demands, including the need for real-time connectivity, fast access to information, and app-based services provided by these devices (Lundgren, 2012; Baldé et al., 2024).

The primary issue with e-waste is its proper disposal and management. Its complex chemical composition varies based on the device's type, model, manufacturer, and

* Corresponding author:
Fabiola Manhas Verbi Pereira
email: fabiola.verbi@unesp.br


https://doi.org/10.31025/2611-4135/2025.19524

production date (Abdelbasir et al., 2018). Improper disposal can cause severe harm to the environment and human health due to the presence of hazardous elements such as Pb in solder, glass panels, batteries, and printed circuit boards (PCBs); Cd in semiconductor chips; Hg in thermostats; and flame retardants in PCBs (Kiddee et al., 2013; Dey et al., 2023).

On the other hand, e-waste recycling offers significant opportunities. Beyond hazardous and toxic components, e-waste contains base metals (Al, Cu, Fe), precious metals (Au, Ag, Pd) from telecommunications and IT equipment, as well as critical elements (In) and rare earth elements (REEs) (Abdelbasir et al., 2018; Baldé et al., 2024). In this context, reverse logistics systems are crucial for promoting the proper management of these materials.

The bibliometric map shown in Figure 1 illustrates the relationships among the 50 most frequently occurring keywords across the 9,175 publications analyzed from 2003 to 2025. The node size is proportional to the number of publications, the line thickness corresponds to the strength of the connection between keywords, and the color of each cluster indicates a grouping of keywords with stronger relationships in the publications (Andrade et al., 2019).

The red cluster encompasses studies on recovering valuable or higher-value-added metals, such as Au and Cu. The green cluster highlights publications addressing the risks to humans and the environment posed by certain substances found in e-waste, such as polychlorinated biphenyls, flame retardants (PBDEs), Cd, Pb, and other potentially toxic metals. The blue cluster encompasses studies on e-waste management and the reuse of recycled and recovered materials. Finally, the yellow cluster includes studies on reverse logistics, sustainability, and the environment.

In developed countries, legislation is more effective and restrictive, with e-waste collected by companies responsible for waste management or government entities and processed through recycling. In contrast, less developed countries often lack adequate infrastructure and legislation, and most waste ends up in open dumps or sanitary landfills, or is incinerated, with little to no separation. In Brazil, projects dedicated to this type of collection are still in their infancy, failing to meet current demand or cover all regional areas of the country (Baldé et al., 2024).

The sectoral agreement requires manufacturers, importers, and distributors to meet collection and disposal targets for EEE sold in the consumer market. Additionally, cities with over 80,000 inhabitants must establish voluntary collection points in easily accessible consumer locations, such as retail stores, educational institutions, and public squares. The federal decree reinforces these targets and emphasizes the implementation of a reverse logistics system for household electronic products, with responsi-

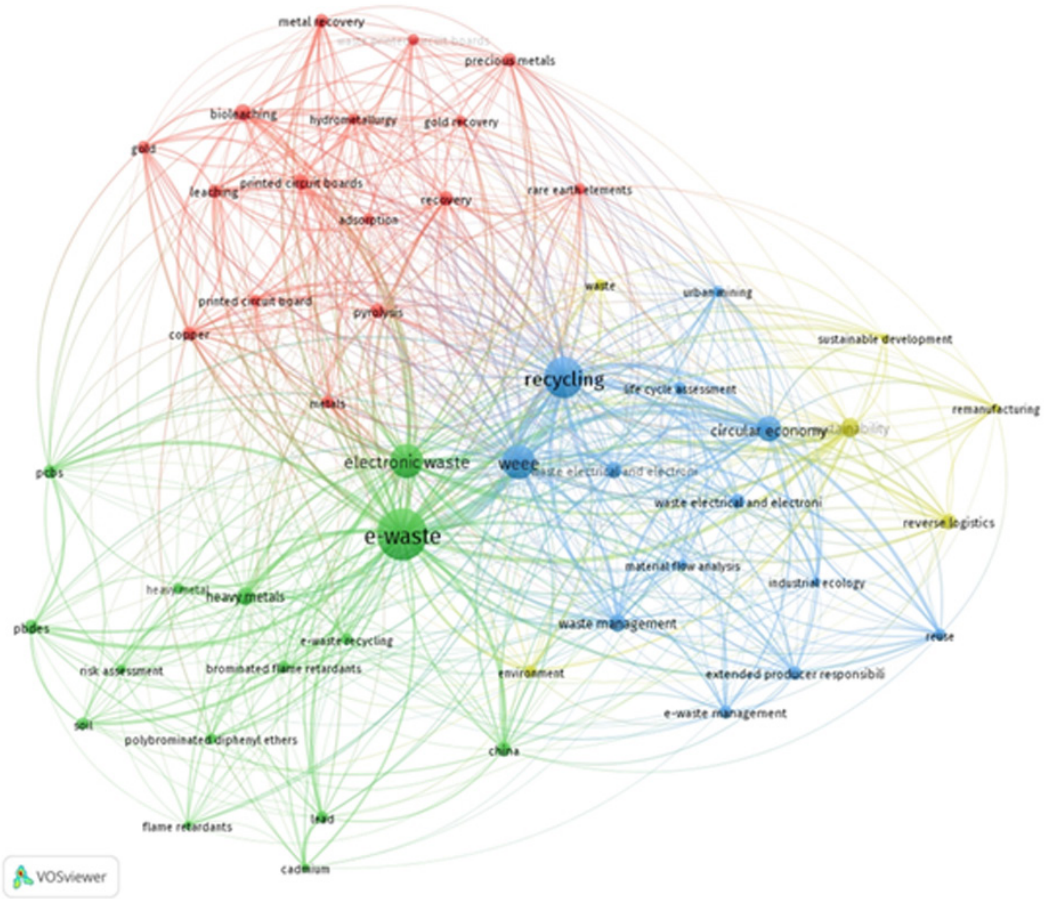


**FIGURE 1:** Bibliometric map generated using the 50 most frequently occurring keywords from 9,175 publications analyzed between 2003 and 2025.

bilities shared among manufacturers, distributors, importers, and retailers (Kiddee et al., 2013; Souza, 2020).

Brazil still faces challenges in collecting these materials. EEE collected properly by licensed companies undergoes a screening process to determine if any items are still usable. Usable items are donated to educational institutions or charities, while non-usable items are classified as waste, dismantled, and separated for value recovery. Specialized companies further process these materials, separating polymers and metals such as Al and Cu. These materials are then sent to other companies to be used as raw materials for manufacturing new products (Souza, 2020).

Although some companies segregate waste, recycling processes capable of transforming waste into new products with high purity levels remain largely inaccessible. As a result, interest in research on this niche continues to grow worldwide (Li et al., 2022).

Our investigation aims to develop a method for evaluating the efficiency of Cu extraction using chemometrics and non-invasive techniques, such as Energy-Dispersive X-Ray Fluorescence (ED-XRF) (Jenkins, 1999) and Laser-Induced Breakdown Spectroscopy (LIBS) (Pereira-Filho et al., 2025). This goal aligns with the principles of Process Intensification (PI), as outlined by Muscetta (2024), which highlights the application of Design of Experiments (DoE) to accelerate decision-making processes in metal recovery. Both analytical techniques can directly analyze solid samples with minimum sample preparation, allowing for the obtaining of complementary results. ED-XRF is capable of determining elements with atomic numbers (Z) greater than 11. Using LIBS, it is possible to obtain analytical signals even for light elements, such as Li, C, and Al (Jenkins, 1999; Pereira-Filho et al., 2025).

## 2. MATERIALS AND METHODS

### 2.1 Sampling and sample preparation

End-of-Life (EoL) computers, laptops, smartphones, and tablets were collected, totaling 12 kg of e-waste. The year of manufacturing varied from 2002 to 2019. These materials were manually disassembled and separated into five parts: polymers, electronic components, cables, metal parts, and PCBs. The PCBs were the primary target samples of this study, which were weighed and processed in a Tecnal TE-650 knife mill (Piracicaba, Brazil). After grinding, the material was sieved until it reached a particle size of less than 212 µm, which was used in the study. At the end of the material preparation process, from collection to obtaining the PCB powder, 1.2 kg of powdered samples were obtained, and destined for the subsequent leaching stages. Table 1 illustrates the 11 experiments performed for each extractor: $HNO_3$, water, and $HNO_3$ combined with NaCl, totaling 33 experiments. In each experiment, a sample mass of around 1.6 g was used. The experiments from 9 to 11 (Table 1) are replicates, and the results obtained were used to compare the analytical techniques.

### 2.2 Chemicals

All solutions were prepared using ultrapure water produced by Milli-Q Plus equipment (Millipore Corp., Bedford, MA, USA). Before use, all glassware and polypropylene bottles were decontaminated with detergent, immersed for 24 hours in a 10% v $v^{-1}$ nitric acid ($HNO_3$) solution (Synth, Diadema, Brazil), and then rinsed with ultrapure water. The reagents used in the leaching processes were analytical grade (P.A.) $HNO_3$ and NaCl (Synth, Diadema, Brazil). Additionally, the concentrated $HNO_3$ was previously distilled using Distillacid BSB-939-IR equipment (Berghof, Eningen, Germany) to ensure the required purity for analysis.

A certified stock standard solution of Cu (1000 mg $L^{-1}$, Specsol, São Paulo, Brazil) was used for the preparation of calibration standards. The detailed procedure for the preparation of the calibration curve is described in Section 2.6.

### 2.3 Leaching procedure

This study conducted metal leaching experiments using three different extractors: (1) 10 mL of 3 mol $L^{-1}$ $HNO_3$,

**TABLE 1:** An experimental design matrix (DoE) with $2^3$ experiments, including a central point (more 3 experiments, 9-11), was used to optimize Cu leaching conditions, and this process was repeated for all three extractors (a total of 33 experiments). The conditions consisted of 10 mL of 3 mol $L^{-1}$ $HNO_3$, 10 mL of water, and 1 mL of 3 mol $L^{-1}$ $HNO_3$ combined with 9 mL of 3 mol $L^{-1}$ NaCl.

| Experiments | Temperature (V1) | | Mixing time every 15 minutes (V2) | | Extraction time (V3) | |
|---|---|---|---|---|---|---|
| | Real (°C) | Coded | Real (min) | Coded | Real (h) | Coded |
| 1 | 25 | -1 | 1 | -1 | 1 | -1 |
| 2 | 70 | 1 | 1 | -1 | 1 | -1 |
| 3 | 25 | -1 | 2 | 1 | 1 | -1 |
| 4 | 70 | 1 | 2 | 1 | 1 | -1 |
| 5 | 25 | -1 | 1 | -1 | 2 | 1 |
| 6 | 70 | 1 | 1 | -1 | 2 | 1 |
| 7 | 25 | -1 | 2 | 1 | 2 | 1 |
| 8 | 70 | 1 | 2 | 1 | 2 | 1 |
| 9 | 47.5 | 0 | 1.5 | 0 | 1.5 | 0 |
| 10 | 47.5 | 0 | 1.5 | 0 | 1.5 | 0 |
| 11 | 47.5 | 0 | 1.5 | 0 | 1.5 | 0 |

(2) 10 mL of water, and (3) 1 mL of 3 mol $L^{-1}$ $HNO_3$ combined with 9 mL of 3 mol $L^{-1}$ NaCl. Three full factorial designs (Table 1) with a central point (experiments 9 – 11) were developed for each extractor, considering the variables temperature of extraction (V1), mixing time (V2, every 15 minutes), and extraction time (V3), as shown in Table 1. A total of 33 experiments were performed.

For Cu leaching using the extractors described earlier, 33 conical tubes (50 mL) were used, and approximately 1.6 g of PCB was weighed into each one. Heating was performed by placing the 33 conical tubes in a block rack set on top of a magnetic stirrer with a heater (model 752A, Fisatom, São Paulo, Brazil), as specified in the experimental design (Table 1). This setup ensured uniform and stable heat transfer to all tubes simultaneously.

In the case of $HNO_3$ 3 mol $L^{-1}$, 10 mL was added to tubes 1 through 11. The Cu leaching is performed according to Equation 1:

$$Cu + 4HNO_3 \rightleftharpoons 2NO_2 + Cu(NO_3)_2 + 2H_2O \quad (1)$$

According to the factorial design, the mixture was agitated at 15-minute intervals. This agitation involved manually vortexing each tube for the specified duration (1, 1.5, or 2 minutes) to ensure complete resuspension of the solid particles. This procedure was based on the conditions evaluated by Dutta et al. (Dutta et al., 2018). After leaching, the solid (inert material) and liquid phases (rich Cu phase) were separated using quantitative filter paper (Unifil, black tape, 125 mm Ø, Germany).

The second leaching was conducted using only water (tubes from 12 to 22). In this case, no leaching process occurs, and the objective was to determine whether the analytical techniques (discussed in detail in the following sections) can effectively distinguish between effective and ineffective extractors. For Cu leaching using $HNO_3$ combined with NaCl, 9 mL of the 3 mol $L^{-1}$ $HNO_3$ solution and 9 mL of the 3 mol $L^{-1}$ NaCl solution were added to tubes numbered 23 to 33. The procedure followed the same experimental conditions as leaching with $HNO_3$, which were based on the parameters studied by Yazici and Deveci (Yazici & Deveci, 2013; Yazici & Deveci, 2015). The study proposed by Yazici and Deveci utilizes Cu ions ($Cu^{2+}$) in combination with $Cl^-$ to form a Cu complex ($CuCl_3^{2-}$), as described by Equation 2:

$$Cu^0 + Cu^{2+} + 6Cl^- \rightarrow 2CuCl_3^{2-} \quad (2)$$

After each leaching, the samples were filtered, and the resulting solid residue was dried in an oven at 40°C until a constant mass was achieved. The liquid phase was separated for further Cu determination using a reference analytical technique described in section 2.6. The following section details the experimental conditions for each leaching strategy evaluated.

## 2.4 LIBS data analysis

After leaching, the obtained solid residues were dried to a constant mass in an oven at 40°C and then manually homogenized. Then, 500 mg of each sample was weighed and pressed in an SSP-10 hydraulic press (Shimadzu, São Paulo, SP, Brazil) with a force of 60 kN for 1 minute, forming pellets with a diameter of 12 mm and a thickness of 2 mm to optimize the instrument's data acquisition. Then, the pellets were directly analyzed using a LIBS system.

LIBS emission spectra were acquired using the LIBS J200 instrument (Applied Spectra, Fremont, CA, USA), which was controlled by the Axiom 2.5 software (Applied Spectra) to configure the operating parameters. The system is equipped with an Nd: YAG laser (Quantel Ultra, Bozeman, MT, USA) with a wavelength of 1064 nm, a pulse duration of 5 ns, and a maximum laser pulse energy of 100 mJ, as well as a 6-channel CCD spectrometer, which records spectral information in the 186 to 1042 nm range. The operating parameters used in this study were a laser pulse fluence of 1,000 J $cm^{-2}$, a spot size of 100 µm, a delay time of 1 µs, and a laser pulse energy of 80 mJ, following previously optimized conditions (Ferreira et al, 2023). The spectra were acquired in a 12 × 12 matrix arrangement, with two pulses applied per point. The spectral data obtained resulted in a 288 × 12,288 matrix, where 288 represents the total number of pulses recorded in the sample, and 12,288 corresponds to the number of emission lines detected within the instrument spectral range (from 186 to 1042 nm).

## 2.5 ED-XRF data analysis

ED-XRF technique was also used to analyze the same solid samples as LIBS. In this case, a benchtop Energy-Dispersive X-Ray Fluorescence (ED-XRF) spectrometer, Rigaku NEX QC+ (Austin, TX, USA), was used to acquire ED-XRF spectra. This instrument features an X-ray tube with an Ag target and a high-performance silicon drift detector, operating at a maximum voltage of 50 kV with an energy resolution of 0.024 keV across 2048 channels. Three distinct instrumental settings were utilized during the analysis: (1) 50 kV and 10 µA, (2) 30 kV and 10 µA, and (3) 6.5 kV and 50 µA, with each measurement conducted over a 30s acquisition time. All spectra were collected under ambient air conditions.

## 2.6 Copper determination to obtain reference values

ICP OES technique was used to obtain the reference concentration values for Cu, utilizing an iCAP 7000 Thermo ICP OES (Thermo Fisher Scientific, Madison, WI, USA). The instrument operated under robust conditions with radial observation, and all measurements were carried out using high-purity argon gas (Ar, 99.999%, White Martins-Praxair). The instrumental conditions employed were: radiofrequency (RF) power of 1.15 kW, plasma flow of 12.0 L $min^{-1}$, auxiliary flow of 0.50 L $min^{-1}$, and nebulizer flow of 0.70 L $min^{-1}$. The integration time varied between 5 and 15 seconds, using a Mira Mist nebulizer and a cyclonic spray chamber. The emission lines monitored for Cu were 324.754 nm, 327.396 nm, and 224.700 nm.

Quantification was performed using an external calibration curve prepared from a certified standard solution of Cu at 1000 mg $L^{-1}$ (Specsol, São Paulo, Brazil), as mentioned in Section 2.2. An analytical curve composed of eleven points was constructed by preparing standards at concentrations of 0.5, 1.0, 2.0, 3.0, and up to 10.0 mg $L^{-1}$.

All standards and the calibration blank were prepared in a 1% v/v $HNO_3$ matrix to match the matrix of the diluted leachate samples. The calibration curve was accepted for analysis only when the linear correlation coefficient ($R^2$) was ≥ 0.999. The method presented a Cu limit of detection (LoD) of 0.006 mg $kg^{-1}$.

### 2.7 Data evaluation

The obtained data were evaluated using MATLAB® 2022b (MathWorks, Natick, MA, USA), Octave (version 8.4.0), and Microsoft Excel for data evaluation, calculations, and statistical tests. Figure 2 summarizes all the steps described previously: sample preparation, Cu leaching processes, and instrumental Cu determination using ICP OES (reference values), ED-XRF, and LIBS.

### 2.8 Analysis of Method Precision

The precision of the instrument and method was evaluated to demonstrate the repeatability of the measurements. For this purpose, data obtained from the center point replicates (n=3, Table 1) were used for each of the four scenarios evaluated: (i) leaching with $HNO_3$ (experiments 9, 10, 11), (ii) leaching with water (experiments 20, 21, 22), (iii) leaching with $HNO_3$ + NaCl (experiments 31, 32, 33), and (iv) the initial sample without leaching. The mean areas (or extraction efficiency), standard deviation (SD),

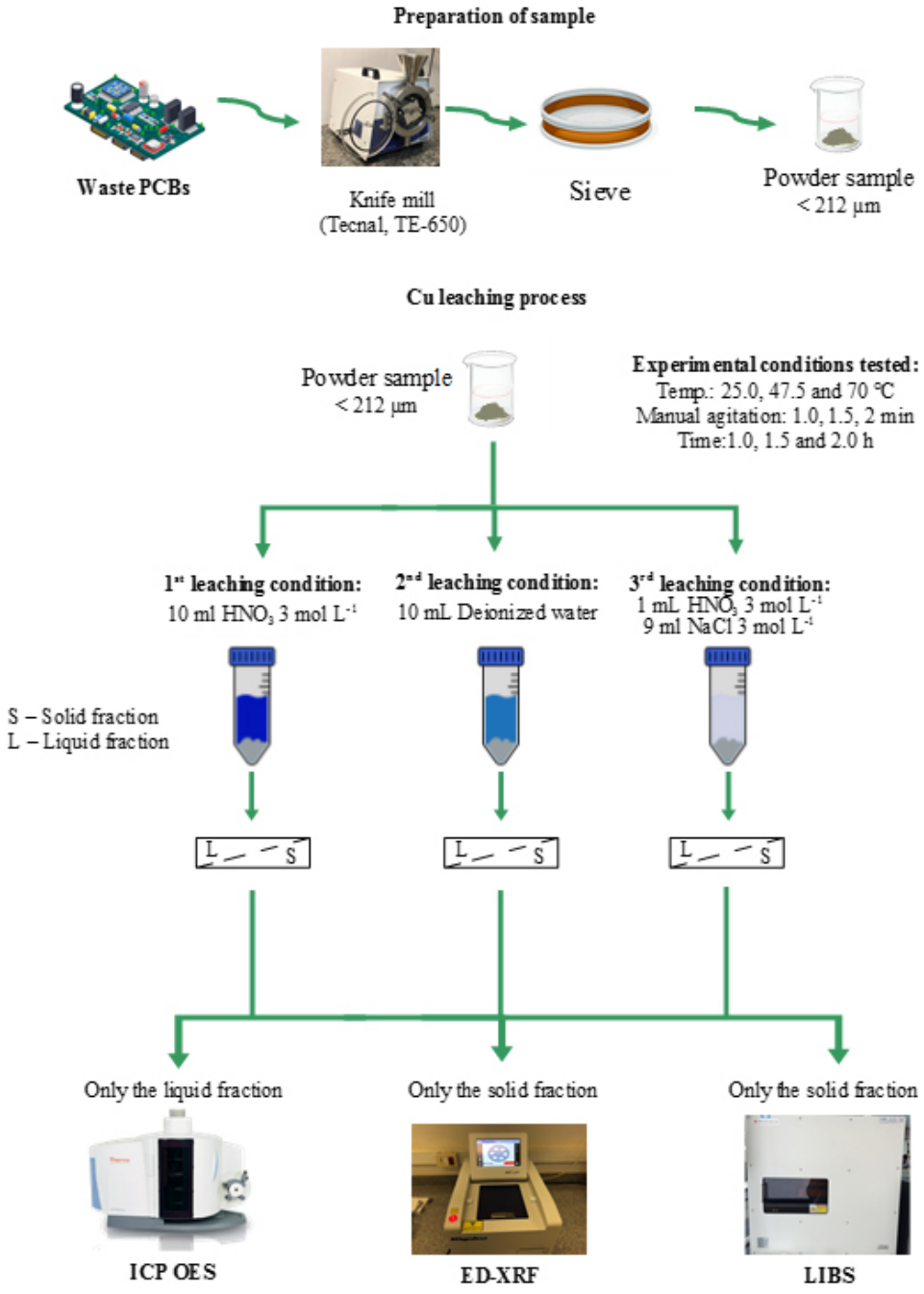


**FIGURE 2:** Description of the experimental procedure for sample preparation and chemical characterization.

and relative standard deviation (RSD = SD/mean x 100) were calculated for the reference analysis by ICP OES, for the Cu Kα signal from ED-XRF, and for the six most relevant Cu emission lines from LIBS.

## 3. RESULTS AND DISCUSSION

### 3.1 Copper reference concentrations using ICP OES

The analytical metric used to evaluate the leaching extraction was the extraction efficiency (EE, %), which is calculated according to Equation 3:

$$EE\ (\%) = \frac{[Analyte\ concentration\ in\ the\ liquid\ extract]}{[Initial\ analyte\ concentration\ in\ the\ solid]} \times 100 \quad (3)$$

The initial Cu mass fraction in the sample was 19% w $w^{-1}$, being obtained after sample preparation using aqua regia (Ferreira & Pereira-Filho, 2025). An excellent EE is close to 100%, which means all the analyte was extracted from the solid to the liquid. Table 2 shows the extraction efficiency (EE) in percentage after Cu determination in the liquid leachates. The EE varied from 0% in the experiments with water (as expected) to 94.8% in experiment 6 with $HNO_3$ 3 mol $L^{-1}$. The experiments with the mixture of $HNO_3$ and NaCl yielded an EE lower than 1%. As noted and expected, the best performance was obtained for the $HNO_3$ 3 mol $L^{-1}$ solution.

ICP OES determinations are often time-consuming and costly. This raises a critical question to be explored in the following sections: Can Cu EE be accurately described using non-invasive, high-throughput analytical techniques such as XRF and LIBS?

### 3.2 Results of first-glance ED-XRF measurements

After obtaining the reference and EE values using ICP OES. The solid residues from each leaching experiment (Table 1) were directly analyzed using ED-XRF. A total of 33 experimental tests were conducted to assess the optimization variations for Cu leaching in the PCB sample and determine the most effective method for evaluating it in future EE estimation.

Figure 3a shows the PCA results (matrix **X** = 33:2048) when considering XRF data. The score values represent the results for Instrumental Setting 1. The best extractor type was $HNO_3$, as indicated by the red symbols over the others. The idea was to provide a scenario with the best leaching conditions for $HNO_3$ (indicated by the red spheres), the worst for $H_2O$ (indicated by the blue spheres), and an intermediate scenario involving $HNO_3$ combined with NaCl (indicated by the pink spheres). The original samples, without extraction (see green spheres), were also used in the calculation to facilitate comparison. The other variables, such as temperature (Figure 3b), mixing time (Figure 3c), and extraction time (Figure 3d), do not influence the clustering of samples, as shown in Figure 3a, because all scores are mixed independently of the experimental condition. The extractor type (Figure 3a) formed two clusters separated by PC1 (94.96%). The negative part of PC1 included samples extracted with $HNO_3$, while the positive part included most of the samples extracted with the other extractors.

The ED-XRF spectra effectively detected Cu as the element with the highest variation, as shown in the loadings depicted in Figure 4. These results indicate that Cu leaching occurred, considering that other relevant x-ray fluorescence lines were Cu Ka at 8.906 keV and Fe Ka and Kb at 6.400 and 7.058 keV, respectively.

The instrumental setting three yields an interesting result: the scores in Figure 5 cluster according to the Cl, as indicated by the loadings in Figure 6. This clustering aligns with positive PC1, being associated with samples leached with $HNO_3$ and NaCl.

### 3.3 Results observed using LIBS

In the case of LIBS, a total of 37 Cu emission lines were previously monitored. Six emission lines were selected: 203.713 nm (ionic emission line denoted as II), 229.384 nm (atomic emission line denoted as I), 282.437 nm (I), 510.554 nm (I), 578.213 nm (I), and 809.263 nm (I); signal areas were then calculated. These emission lines showed the highest correlation (r), with the EE values varying from -0.6637 (for the 578.213 nm line) to -0.6061 (for the 203.713 nm line). As can be observed, the r values are negative, meaning that the higher the EE (i.e., less Cu in the sol-

**TABLE 2:** Extraction efficiency (%) obtained after ICP OES determination for 10 mL of $HNO_3$ 3 mol $L^{-1}$ (experiments from 1 to 11), 10 mL water (from 12 to 22), and 1 mL of $HNO_3$ 3 mol $L^{-1}$ combined with 9 mL of NaCl 3 mol $L^{-1}$ (from 23 to 33).

| Experiments | EE (%) | Experiments | EE (%) | Experiments | EE (%) |
|---|---|---|---|---|---|
| Leachate: $HNO_3$ 3 mol $L^{-1}$ | | Leachate: Water | | Leachate: $HNO_3$ combined with NaCl | |
| 1 | 82.6 | 12 | 0.0 | 23 | 0.0 |
| 2 | 67.8 | 13 | 0.0 | 24 | 0.2 |
| 3 | 79.6 | 14 | 0.0 | 25 | 0.4 |
| 4 | 71.6 | 15 | 0.0 | 26 | 0.5 |
| 5 | 63.1 | 16 | 0.0 | 27 | 0.2 |
| 6 | 94.8 | 17 | 0.0 | 28 | 0.0 |
| 7 | 84.4 | 18 | 0.0 | 29 | 0.2 |
| 8 | 71.8 | 19 | 0.0 | 30 | 0.6 |
| 9 | 68.5 | 20 | 0.0 | 31 | 0.4 |
| 10 | 62.2 | 21 | 0.0 | 32 | 0.3 |
| 11 | 59.0 | 22 | 0.0 | 33 | 0.4 |

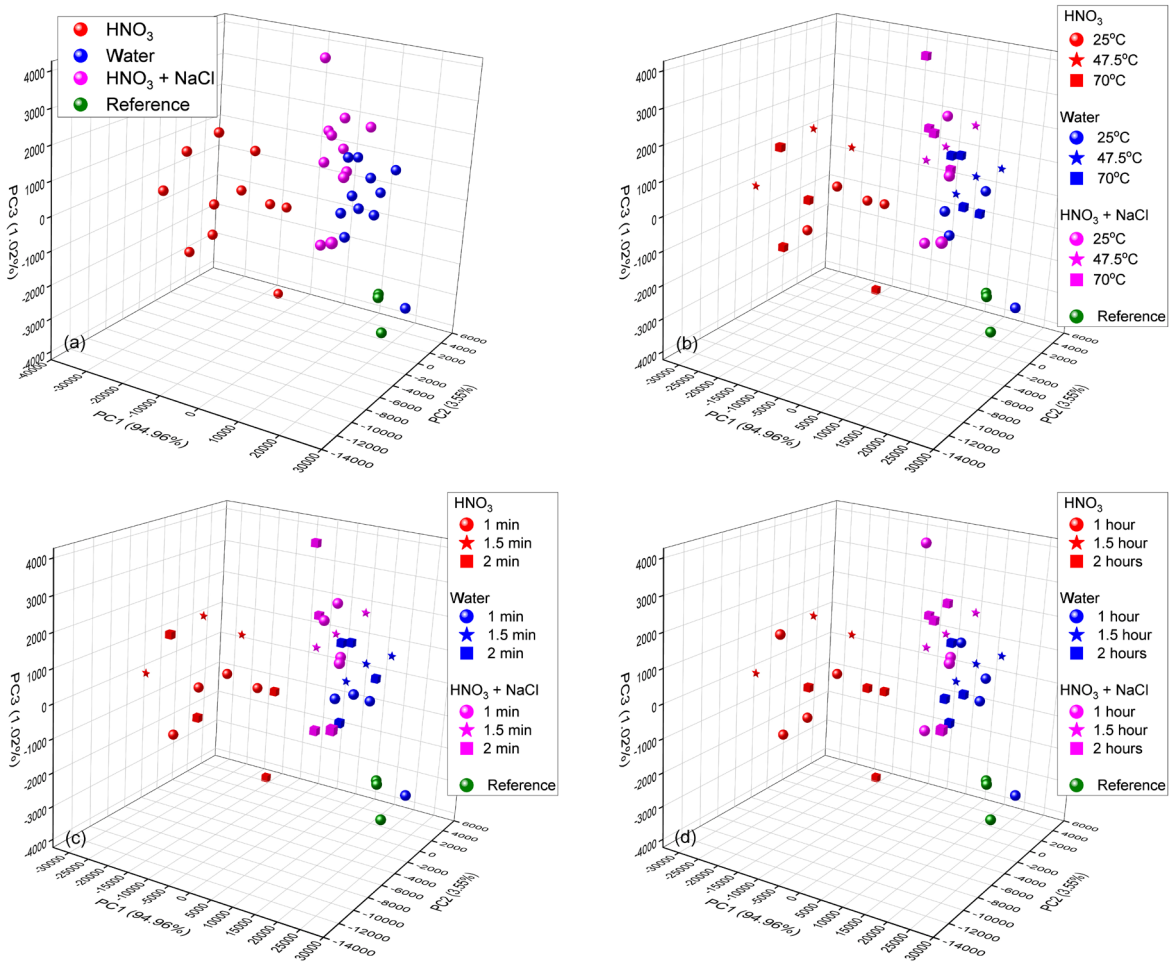


**FIGURE 3:** Score values using instrumental setting one obtained for PCA of ED-XRF: type of extractors (a), temperature (b), mixing time (c), and extraction time (d) for the 11 experiments performed using an experimental design matrix (DoE) with $2^3$ experiments, including a central point.

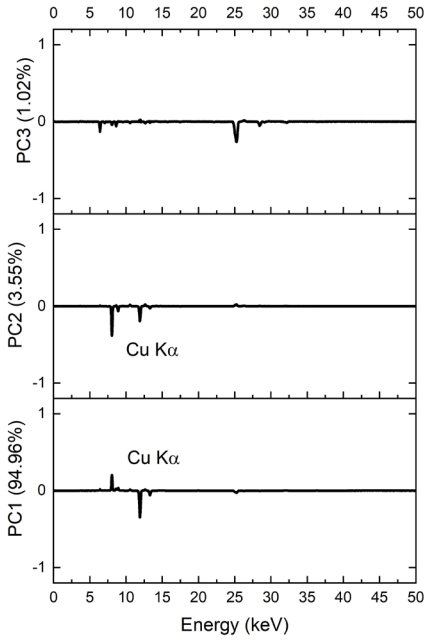


**FIGURE 4:** Loading values for PC1, PC2, and PC3 with Cu Kα highlighted.

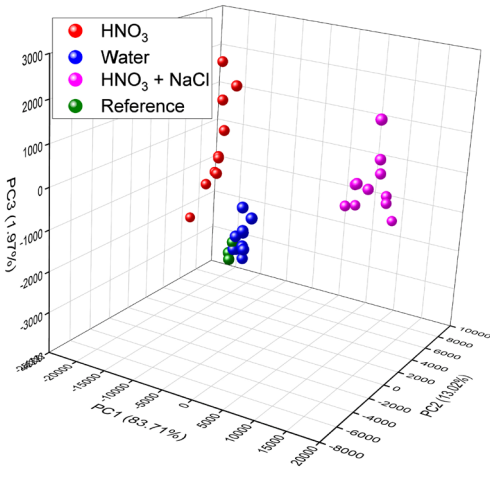


**FIGURE 5:** Score values using instrumental setting three were obtained for PCA of ED-XRF, considering only the type of extractors from the experimental design matrix (DoE) with $2^3$ experiments, including a central point.

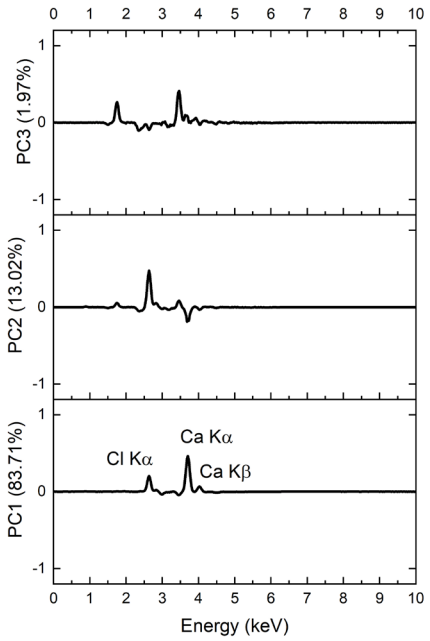


**FIGURE 6:** Loading values for PC1, PC2, and PC3 highlighted for Cl Kα, Ca Kα, and Ca Kβ.

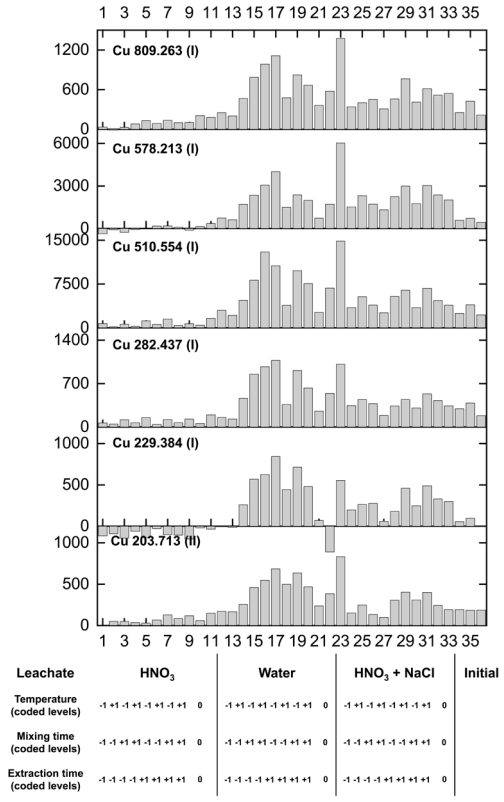


**FIGURE 7:** Cu signal areas for the six emission lines selected from LIBS inspection.

id residue), the lower the areas. Figure 7 shows the signal area for the six lines from the 33 experiments and the three initial samples (34, 35, and 36).

As noted, the samples from 1 to 11, extracted using $HNO_3$, presented the lowest areas of Cu, showing good concordance with the EE, which varied from 59.1% (experiment 11) to 94.8% (experiment 6). Similarly, using XRF, it was impossible to detect a difference in the other variables studied in the DoE. The experiments extracted with water (12-22) presented the highest Cu area.

A PCA was also calculated using the entire dataset (matrix **X** 33:6) after autoscaling. Figure 8 shows the results of the scores (Figure 8a) and loadings (Figure 8b). The samples submitted to $HNO_3$ extraction exhibited different behavior compared to the others. The last evaluation performed was a Tukey test (Christensen, 1996) to confirm differences among the three extractors.

Figure 9 shows the results for the six emission lines described earlier: 203.713 nm (Figure 9a), 229.384 nm (Figure 9b), 282.437 nm (Figure 9c), 510.554 nm (Figure 9d), 578.213 nm (Figure 9e), and 809.263 nm (Figure 9f). A difference was observed between the $HNO_3$ (represented as b) and the other extractors (represented as a) with a 95% confidence level.

### 3.4 Precision analysis and comparative performance

To evaluate the reliability and practical applicability of the proposed non-invasive techniques, a performance analysis was conducted, focusing on both the precision of

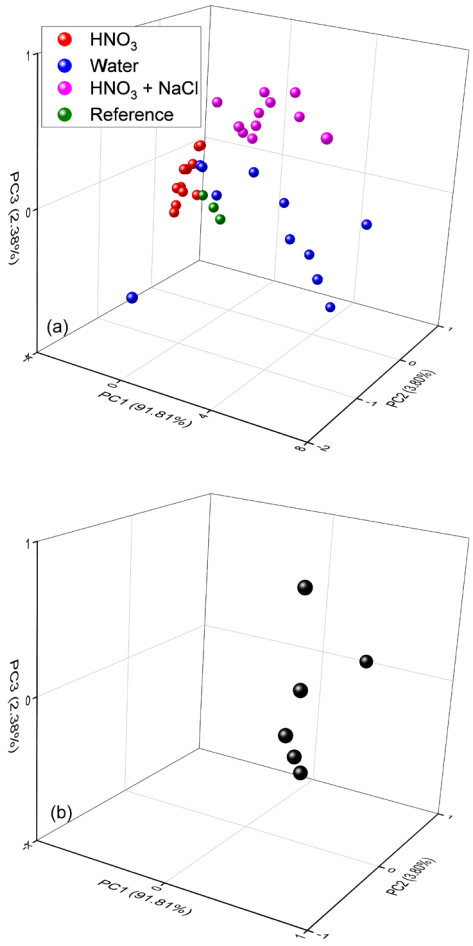


**FIGURE 8:** Score (a) and loading (b) values for the six Cu emission lines selected from LIBS inspection.

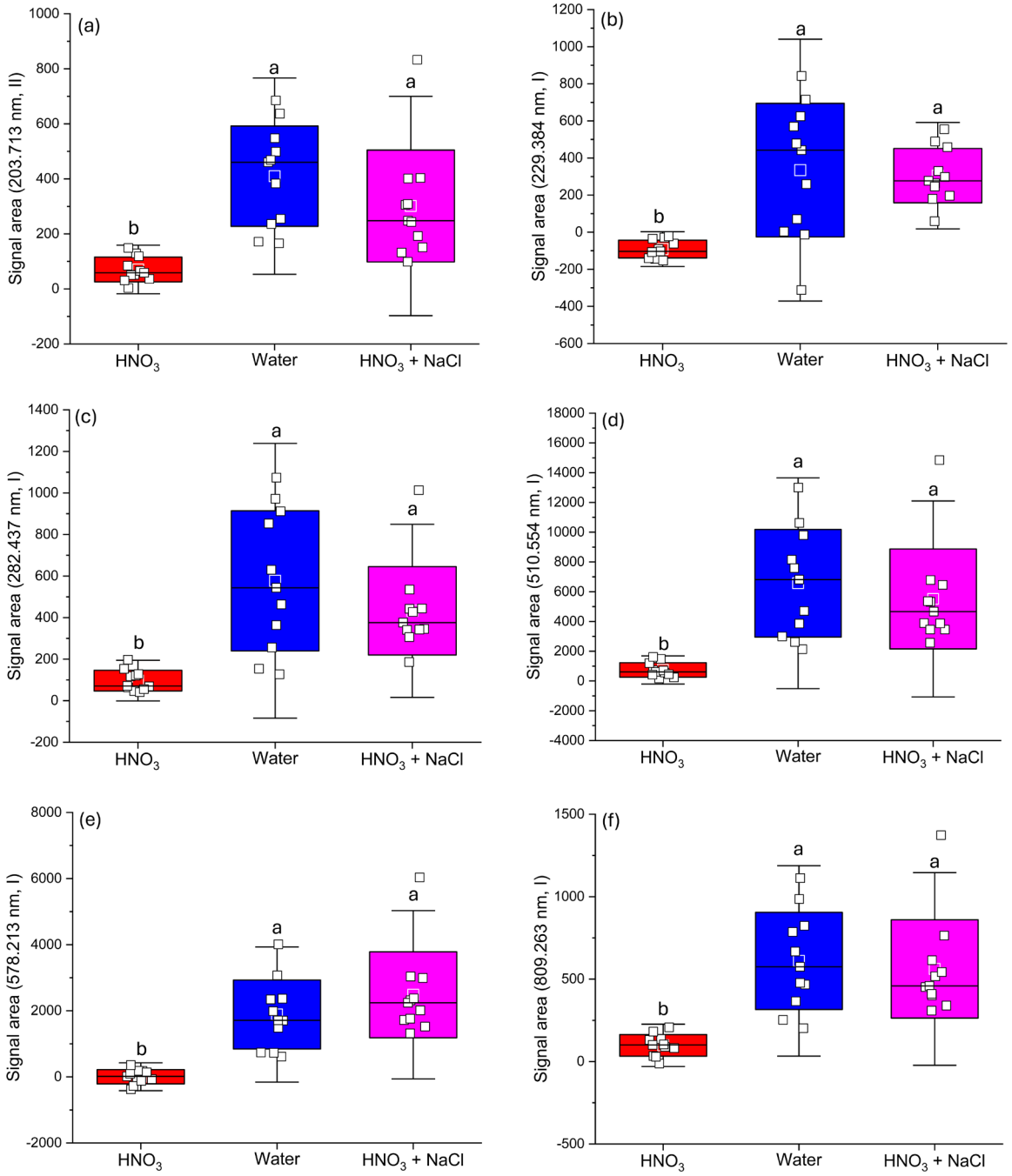


**FIGURE 9:** Tukey tests were performed on the six Cu emission lines selected: 203.713 nm (a), 229.384 nm (b), 282.437 nm (c), 510.554 nm (d), 578.213 nm (e), and 809.263 nm (f). The extractors' water and $HNO_3$ + NaCl are statistically similar (depicted as a) and different from $HNO_3$ (shown as b).

the measurements and the overall performance in comparison with the reference method (ICP OES).

To assess the reliability of each technique, the precision of the measurements was quantified and compared. Table 3 presents the precision data, calculated from the center point replicates (n=3), for the three leaching scenarios (Table 1).

Table 3 provides a basis for comparing the performance of each method. ICP OES, as the reference technique, exhibits excellent precision (4.85), with an RSD of approximately 7.7% for the leaching processes. This value encompasses the variability of the entire experimental procedure (weighing, reaction, filtration, dilution, and measurement), confirming the high repeatability of the developed leaching protocol.

The direct solid analysis techniques, ED-XRF and LIBS, show, as expected, greater variability. For ED-XRF, the RSD of the Cu Kα signal was 37.8% in the low concentration scenario (after leaching with $HNO_3$), an expected increase in variability when measurements approach the limit of detection of an instrument. In contrast, in high Cu concentration scenarios (extraction with water and the mixture

**TABLE 3:** Precision data (mean, Standard Deviation - SD, and Relative Standard Deviation - RSD) for the analytical techniques, estimated from the center points (n = 3) of each matrix from the Design of Experiments (DoE).

| Scenario | Technique | Analyte/Signal | Mean | SD | RSD (%) |
|---|---|---|---|---|---|
| $HNO_3$ Leaching (Effective Leaching, pellets 9-11) | ICP OES | Extraction Efficiency (%) | 63.25 | 4.85 | 7.66 |
| | ED-XRF | Area at Cu Kα | 0.106 | 0.040 | 37.8 |
| | LIBS | Area at 510.554 nm | 923.53 | 609.97 | 66.0 |
| | LIBS | Area at 229.384 nm | -70.05 | 72.57 | -104 |
| | LIBS | Area at 282.437 nm | 126.41 | 70.49 | 55.8 |
| | LIBS | Area at 203.713 nm | 108.55 | 45.87 | 42.3 |
| | LIBS | Area at 578.213 nm | 123.23 | 238.25 | 193 |
| | LIBS | Area at 809.263 nm | 163.85 | 53.89 | 32.9 |
| Water Leaching (Ineffective Leaching, pellets 20-22) | ICP OES | Extraction Efficiency (%) | 0 | 0 | N/A |
| | ED-XRF | Area at Cu Kα | 1.094 | 0.104 | 9.53 |
| | LIBS | Area at 510.554 nm | 5671.31 | 2672.47 | 47.1 |
| | LIBS | Area at 229.384 nm | 78.83 | 395.16 | 501 |
| | LIBS | Area at 282.437 nm | 476.33 | 195.83 | 41.1 |
| | LIBS | Area at 203.713 nm | 362.66 | 117.50 | 32.4 |
| | LIBS | Area at 1475.074 nm | 1475.07 | 662.05 | 44.9 |
| | LIBS | Area at 535.6534 nm | 535.65 | 154.69 | 28.9 |
| $HNO_3$ + NaCl Leaching (Ineffective Leaching, pellets 31-33) | ICP OES | Extraction Efficiency (%) | 0.350 | 0.027 | 7.62 |
| | ED-XRF | Area at Cu Kα | 0.896 | 0.179 | 20.0 |
| | LIBS | Area at 510.554 nm | 5106.42 | 1507.29 | 29.5 |
| | LIBS | Area at 229.384 nm | 372.22 | 102.34 | 27.5 |
| | LIBS | Area at 282.437 nm | 434.73 | 96.27 | 22.1 |
| | LIBS | Area at 203.713 nm | 278.77 | 109.22 | 39.2 |
| | LIBS | Area at 578.213 nm | 2473.40 | 519.46 | 21.0 |
| | LIBS | Area at 809.263 nm | 557.44 | 50.53 | 9.06 |
| Initial Sample (No Leaching, pellets 34-36) | ICP OES | Initial Cu concentration (% w $w^{-1}$) | 19.02 | 3.08 | 16.2 |
| | ED-XRF | Area at Cu Kα | 1.77 | 0.156 | 8.78 |
| | LIBS | Area at 510.554 nm | 2878.88 | 940.26 | 32.7 |
| | LIBS | Area at 229.384 nm | 51.22 | 46.56 | 90.9 |
| | LIBS | Area at 282.437 nm | 287.41 | 101.85 | 35.4 |
| | LIBS | Area at 203.713 nm | 187.54 | 3.26 | 1.73 |
| | LIBS | Area at 578.213 nm | 579.63 | 141.53 | 24.4 |
| | LIBS | Area at 809.263 nm | 297.72 | 112.90 | 37.9 |

of $HNO_3$ + NaCl), precision improves significantly (RSD of 9.5% and 20.0%).

The LIBS, by its nature, shows a variation in precision between different emission lines. The line at 809.263 nm, for example, demonstrated remarkable precision for a plasma analysis technique on solids, with an RSD of only 9.1% in the leaching ($HNO_3$ + NaCl) scenario. It is important to note that the RSD of the 229.384 nm line (-103.6%) was anomalous for leaching with $HNO_3$. This is because the average Cu signal was practically zero, indicating that the extraction was so efficient that the Cu emission on this line reached the background noise of the instrument, a result that, in itself, demonstrates the success of the process.

In general, the precision analysis described each method experimentally. Although ED-XRF and LIBS are less precise than ICP OES in terms of RSD, the magnitude of the change in average area between the different scenarios is adequate. For example, the average area of the XRF signal drops by 90% (from 1.09 to 0.11) after leaching with $HNO_3$. This change, which is much greater than the measurement precision, allows for an adequate evaluation of the process result. Therefore, the data confirm that the repeatability of ED-XRF and LIBS is entirely sufficient for the proposed process monitoring application, offering a fast and low-cost alternative to the reference method.

## 4. CONCLUSIONS

The tested alternative for the in-situ generation of Cu ions in the liquid medium — using an $HNO_3$ + NaCl extractor — did not produce satisfactory results, indicating the

need for further investigations to optimize this approach. Conversely, the findings demonstrate that the analytical techniques evaluated — LIBS and ED-XRF — are effective in differentiating leachates based on Cu signals. Moreover, these methods provide higher analytical throughput and lower operating costs compared to ICP OES. Consequently, they can enhance process understanding and facilitate improved decision-making, particularly when Process Intensification (PI) is integrated with DoE in the context of Cu recycling from Waste Electrical and Electronic Equipment (WEEE).

## ACKNOWLEDGEMENTS

This study was financed, in part, by the São Paulo Research Foundation (FAPESP), Brazil. Processes Numbers #2024/17925-1 and #2019/01102-8, National Council for Scientific and Technological Development (CNPq) grants nos. 302085/2022, 304684/2024-4, and 140867/2021-0, Tertiary Education Trust Fund (TETFund) and the Coordination for the Improvement of Higher Education Personnel (CAPES) - Finance Code 001.

## REFERENCES

Abdelbasir, S.M., El-Sheltawy, C.T., Abdo, D.M., 2018. Green processes for electronic waste recycling: a review. J. Sustain. Metall. 4, 295–311. https://doi.org/10.1007/s40831-018-0175-3

Andrade, D.F., Romanelli, J.P., Pereira-Filho, E.R., 2019. Past and emerging topics related to electronic waste management: top countries, trends, and perspectives. Environ. Sci. Pollut. Res. 26, 17135-17151. https://doi.org/10.1007/s11356-019-05089-y

Baldé, C.P., Kuehr, R., Yamamoto, T., McDonald, R., Althaf, S., Bel, G., Deubzer, O., Fernandez-Cubillo, E., Forti, V., Gray, V., Herat, S., Honda, S., Iattoni, G., Khetriwal, D.S., Luda di Cortemiglia, V., 2024. The global e-waste monitor 2024. United Nations University (UNU)/ United Nations Institute for Training and Research (UNITAR) – co-hosted SCYCLE Programme, International Telecommunication Union (ITU) & International Solid Waste Association (ISWA), Bonn/ Geneva/Rotterdam.

Christensen, R., 1996. Analysis of variance, design, and regression applied statistical methods, Chapman and Hall, New York.

Dey, S., Veerendra, G.T.N., Padavala, S.S.A.B., Manoj, A.V.P., 2023. Recycling of e-waste materials for controlling the environmental and human health degradation in India. Green Anal. Chem. 7, 100085. https://doi.org/10.1016/j.greeac.2023.100085

Dutta, D., Panda, R., Kumari, A., Goel, S., Jha, M.K., 2018. Sustainable recycling process for metals recovery from used printed circuit boards (PCBs). Sustain. Mater. Technol. 17, e00066. https://doi.org/10.1016/J.SUSMAT.2018.E00066

Ferreira, D.S., Pereira-Filho, E.R. 2025. A preliminary study of a sequential leaching process to recover Ag, Au, Cu, and Sn from E-waste 235, 106476. https://doi.org/10.1016/j.hydromet.2025.106476

Ferreira, D.S., Rodrigues, L.S., Pereira, F.M.V., Pereira-Filho, E.R., 2023. Principal component analysis (PCA) para a avaliação de dados químicos e geração de heat maps: um tutorial Quim. Nova 46, 747–754. http://dx.doi.org/10.21577/0100-4042.20230030

Jenkins, R., 1999. X-ray fluorescence spectrometry, 1st ed. Wiley. https://doi.org/10.1002/9781118521014

Kiddee, P., Naidu, R., Wong, M.H., 2013. Electronic waste management approaches: An overview. Waste Manage. 33, 1237–1250. https://doi.org/10.1016/j.wasman.2013.01.00

Li, X., Wu, Y., Tan, Z., 2022. An overview on bioremediation technologies for soil pollution in E-waste dismantling areas. J. Environ. Chem. Eng. 10, 107839. https://doi.org/10.1016/j.jece.2022.107839

Lundgren, K., 2012. The global impact of e-waste: addressing the challenge, International Labour Office, Programme on Safety and Health at Work and the Environment (SafeWork), Sectoral Activities Department (SECTOR), Geneva: ILO.

Muscetta, M., 2024. Process intensification in metal recovery from solid waste: Challenges, opportunities and recent advances. Chem. Eng. Process. 204, 109937. https://doi.org/10.1016/j.cep.2024.109937

Pereira-Filho, E.R., Pereira, F.M.V., Machado, R.C., Andrade, D.F., Babos, D.V., Garcia, J.A., Sperança, M.A., Gamela, R.R., 2025. LIBS analysis of industrial composite materials. In: Galbács, G. (eds) Laser-induced breakdown spectroscopy in biological, forensic and materials sciences. Springer, Cham. https://doi.org/10.1007/978-3-031-85975-5_20

Souza, R.G., 2020. E-waste situation and current practices in Brazil, in: M. L. Ogunseitan (Ed.), Handbook of electronic waste management, 1st ed., Elsevier, pp. 399-417. https://doi.org/10.1016/B978-0-12-817030-4.00009-7

Yazici, E.Y., Deveci, H., 2013. Extraction of metals from waste printed circuit boards (WPCBs) in $H_2SO_4$–$CuSO_4$–NaCl solutions. Hydrometallurgy 139, 30-38. http://dx.doi.org/10.1016/j.hydromet.2013.06.018

Yazici, E.Y., Deveci, H., 2015. Cupric chloride leaching (HCl–$CuCl_2$–NaCl) of metals from waste printed circuit boards (WPCBs). Int. J. Miner. Process. 134, 89-96. http://dx.doi.org/10.1016/j.minpro.2014.10.012